Bicycle disc brake noise analysis and mitigation

Singh, Ajaypal; Vreman, Hans; Dressel, Andrew E.; Moore, Jason K.

DOI
10.1177/10775463241273021

Publication date
2024

Document Version
Final published version

Published in
JVC/Journal of Vibration and Control

Original Manuscript

Journal of Vibration and Control
2024, Vol. 0(0) 1–10

DOI: 10.1177/10775463241273021
journals.sagepub.com/home/jvc
Sage

Bicycle disc brake noise analysis and mitigation

Ajaypal Singh[1], Hans Vreman[2], Andrew E Dressel[3], and Jason K Moore[1]

Abstract

This project was designed to understand the causes and mechanisms of bicycle disc brake noise and use that information to formulate and evaluate possible mitigation techniques. Brake noise was generated by a real bicycle running on a treadmill and recorded by microphone and laser vibrometer. Six independent variables, brake force, rotor thickness, front fork stiffness, weather conditions, spoke tension, and friction coefficient, were varied according to a one-quarter fractional factorial design. A finite element model of the rotor, pads, and calliper was also formulated and analysed. The results of these two methods, particularly the disc mode shapes and frequencies, suggest that doublet mode splitting and re-converging plays a role in noise generation and that changing the rotor mass or breaking its symmetry could interfere with such noise generation. Finally, of these mitigations, breaking disc symmetry proved the most fruitful, with noise magnitude reductions from 72% to 99%, depending on frequency.

Keywords

bicycle, disc, brake, noise, generation, mitigation

1. Background

In addition to environmental issues, brake noise also adversely affects brake and bicycle manufacturers. Brake manufacturers spend around 50% of their R&D budget on brake noise and vibration issues, and these issues are responsible for more than half of their after-sales service expenses (Abendroth et al., 2000). Brake manufacturers can also suffer from economic penalties because of warranty claims or the perception of reduced quality and hence a negative brand image among consumers.

This research investigates only noise generated by bicycle disc brakes, and there are several phenomena involved in the generation of this noise (Singh 2022). One is 'stick-slip', in which the brake pads alternately stick to and then slip over the rotor. The exact mechanisms by which stick-slip occurs are an active area of research, but the details are not necessary here.

Another phenomenon is called 'mode lock-in', by which the vibrational modes of two different sub-structures with similar natural vibration frequencies couple together, which results in a 'resonant-like response' and leads to an increase in the vibration amplitudes (Allgaier et al., 1970).

Allgaier et al., citing Akay, enumerate three distinct types of mode lock-in that can be present in a system. Classical mode lock-in occurs when the modes of the components have nearly identical eigenfrequencies and thus a lock-in occurs at that frequency. Intermediate mode lock-in occurs when the system locks into a frequency that lies in between the Eigenfrequencies of the components. Multiple mode lock-in occurs when doublet modes (defined below) are present simultaneously along with other types of lock-in in a system. In multiple lock-in, the noise spectrum not only consists of one dominant frequency and its harmonics but also the sidebands.

A doublet mode is present when two Eigenmodes with the same nodal circles (circles of points on the disc that do not move with the mode) and diameters (straight lines of points through the centre of the disc that do not move with the mode) and have similar frequencies but different phases. Splitting of doublet modes, or flutter instability theory, was first presented by Mottershead and Chan (Chan et al., 1994).

[1]Department of BioMechanical Engineering, Delft University of Technology, Delft, The Netherlands
[2]Royal Dutch Gazelle N.V., Dieren, The Netherlands
[3]Department of Civil Engineering, University of Wisconsin-Milwaukee, Milwaukee, WI, USA

Corresponding author:
Andrew E Dressel, Department of Civil Engineering, University of Wisconsin-Milwaukee, 3200 N Cramer St, Suite 503, Milwaukee, WI 53201-0413, USA.
Email: ADressel@uwm.edu

They noted that in a symmetric rotor, a single Eigenmode can split into a pair of doublet modes. This splitting of modes can lead to flutter which results in noise. Lang et al. and Nishiwaki et al. in their separate studies of brake noise observed doublet modes (Lang et al., 1993; Nishlwakl et al., 1989). They performed studies to investigate these modes and concluded that doublet modes often converge together during vibration and induce system instabilities.

In summary: symmetrical structures have a tendency for their Eigenmodes to split into a pair of doublet modes with the same mode shape and then converge back together causing a flutter instability in the system.

We examine bicycle disc brake noise by measuring the mode shape with a laser vibrometer, capture the audible frequencies with a microphone, and develop a finite element simulation that identify and cross verify the presence of doublet modes for several brake calliper and pad combinations in wet and dry conditions. We close with an example noise mitigation measure since doublet modes are tied to symmetry.

2. Experiment design

We investigate brake noise with six different possible causal conditions, as shown in Table 1. For simplicity and to reduce the number of test runs, we used one-quarter fractional factorial design. The six independent variables whose values we could control in the laboratory settings to test the brake noise are shown in Table 1 below. In most cases, the values come directly from the equipment tested: a thick rotor and a thin one, a stiff fork and a less stiff fork, higher friction brake pads and lower friction pads. The spoke tension values are the rim manufacturer's upper and lower limits.

We could not control the other variables, such as wear in the pads, wear in the rotor, and brake system mass, and we therefore left them out of the analysis. We tested every variable at two levels: high and low. The high level denoted by '+1' consisted of a higher value of the independent variable, and the lower level denoted by '-1' consisted of a lower value. The rows in the design matrix (Table 2) represent the experimental runs and the levels of variables for each run.

3. Experimentation

We captured brake noise magnitude with a BOYA BY-M1 microphone and mode shapes of the rotor, calliper, and fork by interferometry for all 16 runs in the design matrix. We simulated braking scenarios in the lab on a brake test machine, which consisted of the bike with the frame and rear wheel fixed while the front wheel rotated on the motor-driven flywheel. We placed a microphone close to the rotor-pad interface to capture the brake noise, and ran the machine at a constant speed of 5 km/hr.

Table 1. Factors to vary with their high and low values.

Factor	Variable	+1	−1
Brake force	A	80 N	40 N
Rotor thickness	B	2 mm	1.8 mm
Front fork stiffness	C	180 N-m/°	154 N-m/°
Weather conditions	D	Wet	Dry
Spoke tension	E	1.4 & 0.98 kN	1.1 & 0.78 kN
Friction coefficient	F	0.22	0.28

We used a similar physical setup for the interferometric measurements, except that the front wheel ran freely on a treadmill, and we fixed the rear wheel and bike frame on a trainer. We used a Polytec PSV-400 vibrometer to measure the vibration velocities and displacements of the rotor, calliper, and front fork without contact. From the collected data, Polytec PSV software performed experimental modal analysis (EMA) 'by fitting a mathematical model to' the 'physical measurement results' (Polytec 2024). This generated one mode shape, shown below in Figures 2–4, for each of the three peak frequencies shown below in Figure 1.

4. Experimental results

We processed the brake noise audio recordings in MATLAB to plot magnitude versus frequency. We observed a clear trend of peak magnitudes, reported in volts, at just three frequencies in all 16 test runs. The peak magnitudes changed with changes in the 6 parameters of the design matrix, but the frequencies at which they occurred remained approximately the same. Figure 1 shows the three frequencies of peak magnitudes, (550–650 Hz), (1100–1300 Hz), and (1650–1950 Hz), and the ratio between frequencies remained constant in all runs: always 1:2 between the lower two frequencies and 2:3 between the higher two frequencies. We saw very similar results in the magnitude versus frequency plots of the vibrometer data, except that it reports magnitude in mm/s.

Results of testing and influence of various factors on noise magnitude at the three frequencies are shown below in Table 3.

5. Discussion

Analysis of the brake noise audio recordings reveals that during a brake noise event we hear three peak frequencies, which remained fairly consistent around 590 Hz, 1180 Hz, and 1770 Hz. We also found that the low frequency noise magnitude during dry conditions was significantly higher than during wet conditions. One possible cause of this noise magnitude change in low frequency can be attributed to the temperature change that might happen at the sliding interface of the rotor and the pads due to the presence of water.

Table 2. One-quarter fractional factorial design matrix with rows as the Test runs and the columns as the variable levels.

	Run	1	2	3	4	5	6	7	8	9	10	11	12	13	14	15	16
Variables	A	−1	1	−1	1	−1	1	−1	1	−1	1	−1	1	−1	1	−1	1
	B	−1	−1	1	1	−1	−1	1	1	−1	−1	1	1	−1	−1	1	1
	C	−1	−1	−1	−1	1	1	1	1	−1	−1	−1	−1	1	1	1	1
	D	−1	−1	−1	−1	−1	−1	−1	−1	1	1	1	1	1	1	1	1
	E	−1	1	1	−1	1	−1	−1	1	−1	1	1	−1	1	−1	−1	1
	F	−1	−1	1	1	1	1	−1	−1	1	1	−1	−1	−1	−1	1	1

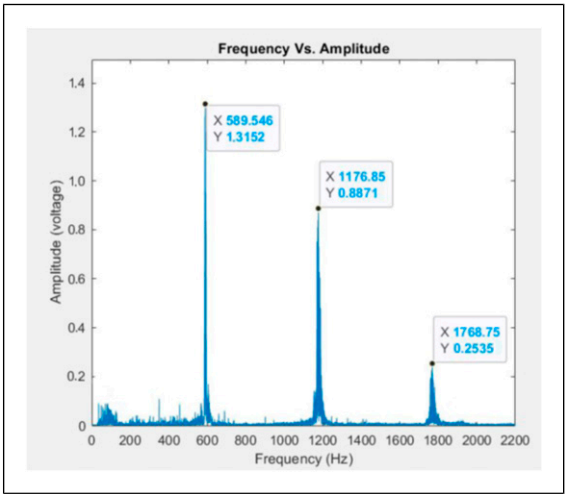

Figure 1. Amplitude versus frequency of the recorded brake noise revealing peaks at three frequencies. Amplitude is in volts, as recorded by the smartphone connected to the BOYA BY-M1 microphone.

The water might lower the temperature at the sliding interface by the process of evaporation. We did not study temperature dependence, however, in this project.

The vibrometer recordings shed light on both the brake noise and no-noise events. For the brake noise events, the vibrometer magnitude versus frequency plots correlated highly with the audio amplitude versus frequency plots, which shows that the brake components are vibrating at the same frequencies as the noise that an observer hears. There were also some decorrelations between noise measured by the microphone and out-of-plane vibration magnitudes measured by the vibrometer. Most notably, low frequency noise was higher in dry conditions, but vibration magnitudes were higher in wet conditions. We did not investigate this decorrelation further.

We observed that during the brake noise events, the rotor vibrated the most at more than 1.5 mm/s, the calliper vibrated at a little less than 1.5 mm/s, and the front fork vibrated at 0.4 mm/s. This confirms that the rotor-pad interface is indeed the source of the vibrations. The vibrations originate from the sliding interface and propagate from the brake system to the hub and from the hub to the front fork. The vibration magnitudes decrease as they travel away from the source, as captured by the vibrometer. Therefore, during the brake noise events, the entire bike vibrates at three peak frequencies, but the sound is emanating from the pad-rotor sliding interface.

We also observed that the maximum out-of-plane (perpendicular to the plane of the disc) vibrations for the bicycle components lie in the low frequencies (550–650 Hz) and were less in the middle and high-frequencies under both wet and dry conditions. . This indicates that higher frequency vibrations do not propagate throughout the brake assembly as much as lower frequency vibrations.

The mode shapes of the fork had less twist and more out-of-plane motion at low frequencies and more twist and less out-of-plane motion at high frequencies. This suggests that during a brake noise event, the fork vibrates both in the bending and torsional directions. The fork also did not have significant vibration amplitudes at higher frequencies.

We found the vibration amplitudes to be higher during wet conditions than dry in all three frequency regions, despite the reduction in noise amplitudes at low frequency discussed above. Also, during dry conditions, the brake noise generation was rather random and certain test runs did not produce any brake noise at all.

To investigate why certain braking events were noisier than others, we estimated a dynamic friction coefficient between the pads and the rotor from the braking distance 's' and braking force 'N' recorded by the brake test machine along with the initial velocity, final velocity, rotor and wheel radii, and wheel polar moment of inertia.

We found the dynamic friction coefficient to be decreasing with an increase in the bicycle running velocity. This observation suggests the likelihood of stick-slip as one of the causes of friction-induced vibration (Rabinowicz 1965). Stick-slip can also explain why the brake noise is consistent during the wet conditions and inconsistent during dry conditions. During wet conditions, a film of water develops between the sliding surfaces, which leads to a reduction in the friction coefficient (Wu-Bavouzet et al., 2007). During dry conditions, the drop in friction coefficient is not as consistent. Therefore, the brake noise events occur when stick-slip causes vibrations in the brake system and the no-noise events are the dry events where the stick-slip is absent.

Table 3. Percentage contributions (%) from the estimated effects matrix for the one-quarter fractional factorial design. Contributions >= 10% are highlighted, and we have excluded columns containing no values >=10% for brevity. Percentage contribution is calculated according to the fractional factorial design statistical analysis described by Montgomery (Montgomery 2017).

Factor	B	C	D	F	AE + BC + DF	AF + DE
550–650 Hz	0.09	0.21	15.0	36.4	30.2	1.08
1100–1300 Hz	0.07	1.19	32.2	11.9	13.4	26.7
1650–1950 Hz	11.4	14.2	0.01	23.9	19.5	12.9

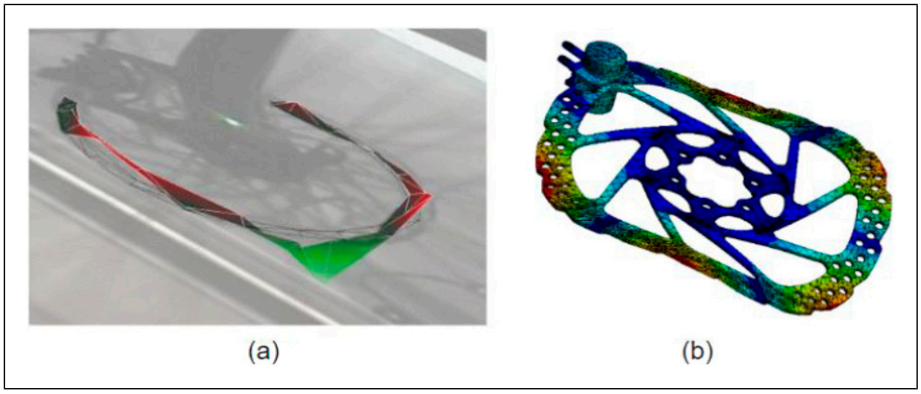

Figure 2. Mode shape (2,1) in the low frequency range (a) at 591 Hz in the physical experiment and (b) at 545 Hz in the FE analysis.

6. Finite element simulation design

We created a reduced FE model comprising only a rotor, brake pads, and the calliper to recreate the observed behaviour described in the prior experiments. We modelled the rotor and brake pads as closely as possible to the physical parts, but we simplified the calliper model significantly. Unlike the rotor and brake pads, the calliper model has few geometric similarities to the physical part used in the experiments. It does not have the intricate details such as shims, bolts, pins, pistons seals, mounting brackets, biasing member, actuation unit, pad axle, hydraulic through holes, and hydraulic connections. Instead, it comprises only a calliper body and two pistons. The material properties specified for the rotor, brake pads, and the calliper also differed a bit from the physical components.

We also limited the degrees of freedom of brake components for simplicity and computational purposes. We allowed the brake pads only to move in the direction normal to the brake pad surface to allow the pads to travel along with the piston as the piston presses against them. Although it is well documented that a change in the centre of pressure (COP) at the brake pad can alter the brake noise propensity and generation (Budinsky et al., 2021), we applied the constraints to its leading and trailing edges to ensure a constant pressure distribution at the pad-rotor interface.

Frictional heating is one of the by-products of the sliding between the rotor and the brake pads. This is known to increase the friction coefficient, and this can contribute to the instabilities in the pad-rotor interface. Moreover, improper energy balance, which this model fails to capture, also affects brake noise generation.

We identified stick-slip as one of the causes of vibrations during the experimental investigation. Even though the pre-stress analysis includes the frictional sliding contact of the pad and rotor, it fails to incorporate the stick-slip effect in the model.

The entire brake assembly is shown in Figures 2–4. We performed pre-stress modal analysis via the Newton–Raphson method in ANSYS to solve the asymmetric matrices produced due to the frictional sliding. The addition of a stress matrix to the stiffness matrix in the base stress analysis made the structural system non-linear, which ANSYS converted to a linear system and then calculated the mode shapes and natural frequencies. We considered natural frequencies up to 2 kHz because we saw from the experiments that the range of brake noise for the bicycle brake system is 0–2 kHz.

7. Finite element simulation results

We observed a total of nine Eigenmodes in the finite element simulations, as shown in Figure 5. These include six unique mode shapes (modes 1, 3, 4, 6, 7, and 9), two of which (modes 4 and 9) are in the plane of the disc. The remaining three (modes 2, 5, and 8) are doublets. In disc

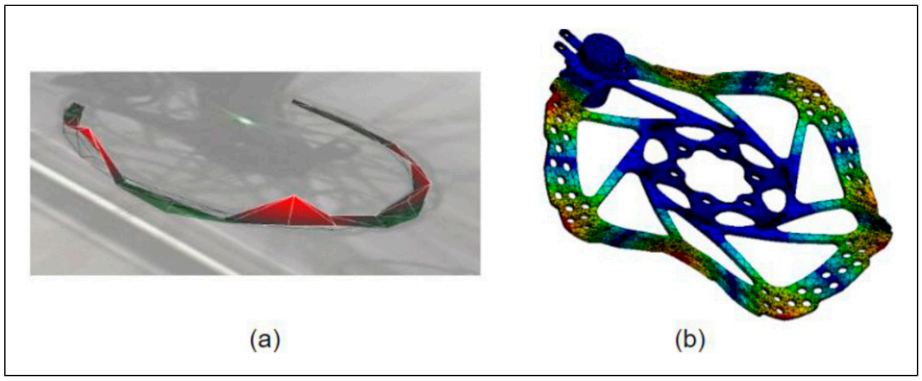

Figure 3. Mode shape (3,1) in the middle frequency range (a) at 1190 Hz in the physical experiment and (b) at 1167 Hz in the FE analysis.

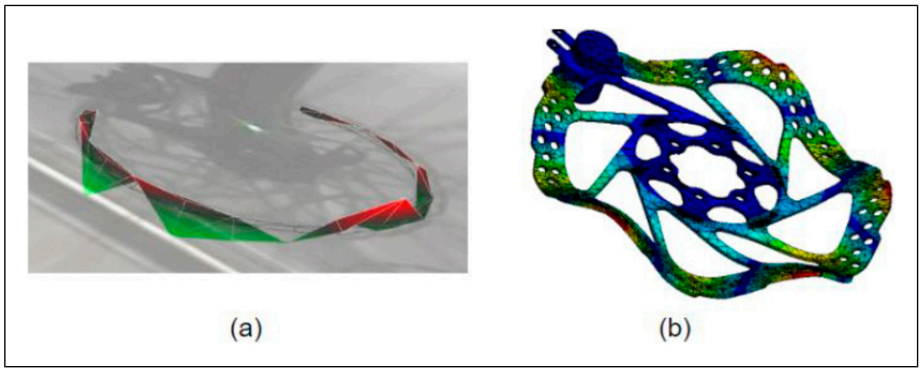

Figure 4. Mode shape (4,1) in the high-frequency range (a) at 1786 Hz in the physical experiment and (b) at 1827 Hz in the FE analysis.

mode shape nomenclature, the first number is the number of nodal diameters, and the second number is the number of notal circles. As indicated in Figure 5, modes 1 and 2 form a doublet pair. They have the same mode shape (2,1) but different phases. Similarly, modes 3 and 5 form a second doublet pair with mode shape (3,1), and modes 6 and 8 form a third with shape (4,1).

We observed only one mode with a frequency in the low range, and it vibrated out-of-plane at 545 Hz, as shown in Figure 2(b).

We observed two modes in the medium frequency range and within 100 Hz of each other. One vibrated out-of-plane 1167 Hz and the second vibrated in-plane at 1072 Hz, as shown in Figure 3(b).

In the high-frequency range, we observed three Eigenmodes vibrating at 1811 Hz, 1830 Hz, and 1864 Hz. The first two were out-of-plane, but only the second one, at 1830 Hz corresponds with a mode observed by the laser vibrometer, and the third was in-plane, as shown in Figure 4(b).

8. Comparison of the experimental and finite element results

The Eigenmodes found by the two types of analysis correlate well and are quite similar. While the physical experiments provide only the end results, the finite element analysis suggests possible causes of what was observed experimentally.

From the physical experiments, we observe that there existed only three frequencies with peak magnitudes during the brake noise events, but the finite element simulations show the presence of more than three frequencies in the assembly. One of the reasons for this difference is that the in-plane modes were not studied experimentally and were observed only in the finite element study. Also, no doublet modes were observed in the physical experiments.

Not only were the mode shapes between the two types of analysis similar, but the frequencies from the finite element modal analysis also match well with those from the experimental analysis. The small differences in the frequencies between the experimental and the analytical analysis can be attributed to the limitations of the finite element analysis discussed in the previous section. Thus, the FE model appears useful for brake noise analysis. Mode shapes and frequencies from the two methods are summarized below in Figure 5

9. Countermeasure design

Based on the observations made during the literature study, experimental investigations, and finite element analysis, we

Mode	Experiments	Mode	FEA	Mode Shape	Mode Shape Interpretation	% Difference
1	**591 Hz**	1	**545 Hz**	(2,1)	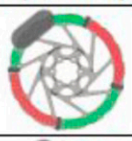	7.70%
	-	2	732 Hz	(2,1)	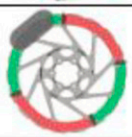	-
	-	3	945 Hz	(3,1)		-
	-	4	1072 Hz	In-plane	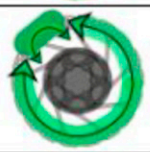	-
2	**1190 Hz**	5	**1167 Hz**	(3,1)		2%
	-	6	1510 Hz	(4,1)	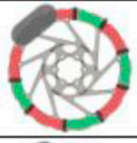	-
	-	7	1811 Hz	(0,2)		-
3	**1786 Hz**	8	**1827 Hz**	(4,1)		2.30%
	-	9	1864 Hz	In-plane	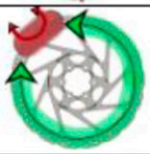	-

Figure 5. Summary of the experimental and FEA mode shapes, eigenfrequencies, and the interpretation of the mode shapes; grey areas are the nodes, and the green and red areas are the positive and negative out-of-plane displacements.

devised three countermeasures to reduce the brake noise magnitude. We tested these countermeasures experimentally on the brake test machine and also by FEA.

Adnan Akay's comprehensive work on frictional acoustics brought to our attention the roll of heat build-up in noise generation (Akay 2002). Automobile brake manufacturers address this issue by splitting the friction lining of their brake pads into sections with various slots. Thus, our first countermeasure was to add a radial slot in the friction lining of the brake pads.

Next, modal analysis of the components revealed that the rotor and the brake pads had similar Eigenfrequencies. This suggests the existence of intermediate mode coupling, which can cause an increase in the vibration amplitude. Thus, our second countermeasure was to increase the mass of the rotor symmetrically, which we expected to decrease

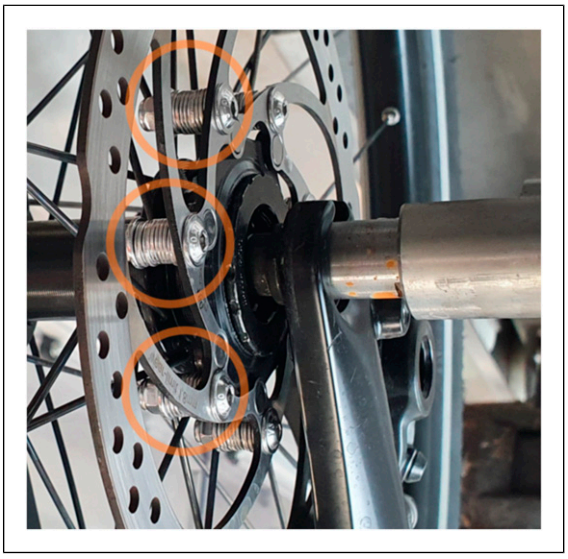

Figure 6. Nuts, bolts, and washers added to all seven ribs of the rotor to increase its overall mass and decrease its natural frequency.

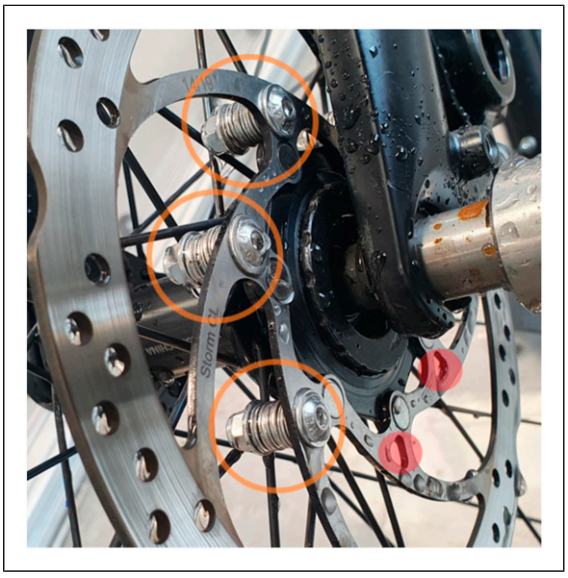

Figure 7. Nuts, bolts, and washers added to only four ribs on one side of the rotor to cause an asymmetric mass distribution; orange circles highlight the additional masses and red dots highlight absences.

its Eigenfrequency and interfere with intermediate mode coupling.

To accomplish this, we formed 9-g bodies, each with a nut, a bolt, and 10 washers, and added seven such bodies to each of the seven rotor ribs, as shown in the Figure 6. This increased the overall mass of the rotor by 30% from 215 g to 278 g.

The Shimano rotors we used for the first experiments did not have room for adding masses, so we switched to Magura MT4 calliper and a Magura STORM CL rotor. We did use the same Gazelle Medeo T10 HMB bicycle with stiffer Suntour NEX E25 HLO front fork, ran the brake test machine at 5 km/h under wet conditions, and applied 80 N to the break lever, but we did not check the spoke tension nor the brake pad coefficient of friction.

Finally, we observed doublet modes in the finite element simulations. These modes lie very close together in the frequency spectrum and often converge together to introduce system instabilities. The literature contains various ways to separate these doublet modes. Lang et al. added mass along the outer circumference of a drum brake, and Nishiwaki et al. altered the number of stiffeners on a ventilated automotive rotor to separate the doublet modes (Lang et al., 1993; Nishlwakl et al., 1989). The effect of rotor symmetry plays a huge role in the appearance and convergence of these doublet modes in the structure. Thus, our third countermeasure was to increase the mass of the rotor asymmetrically to counter this.

We introduced asymmetry by adding 9-g masses, just as in the symmetric loading, but to ribs on only one half of the rotor, as shown in Figure 7, and which increased the overall mass of the rotor by 17%. Note that 4, 9-g masses do amount to 36 g, but they are mounted at a radius of about only 25 mm, and their combined centre of mass is at an even smaller radius. For comparison, aluminium presta valve stems have masses of 8, 9, or 10 g, depending on length, and they are mounted on the rim with a radius of about 300 mm. Thus, the unbalanced force, calculated as $mr\omega^2$, of the lightest presta valve would be at least 2.7 times larger than the unbalanced force generated by our crude modification.

10. Countermeasure results

Each countermeasure reduced brake noise to varying degrees, as shown in Figure 8 below. Although the brake noise magnitude decreased by a considerable amount, the brake noise frequencies remained fairly unaffected.

Although we did oberve that the slots successfully suppressed brake noise, as shown in Table 4, we did not investigate any change in braking performance they may have created.

Symmetric loading was very effective at reducing the brake noise magnitude, and it also decreased the frequencies a bit. Figure 8 displays the brake noise audio results for the symmetric loading in comparison with the reference runs and other countermeasures. Table 5 shows the difference in the magnitude and frequency of the brake noise between the reference run and the symmetrically loaded run. It caused reductions of 75% in low frequency magnitude, 55.7% in middle frequency magnitude, and 63% in high-frequency magnitude. It also reduced middle frequency and high-frequency vibrations by an average 24.2 Hz and 33.8 Hz, respectively.

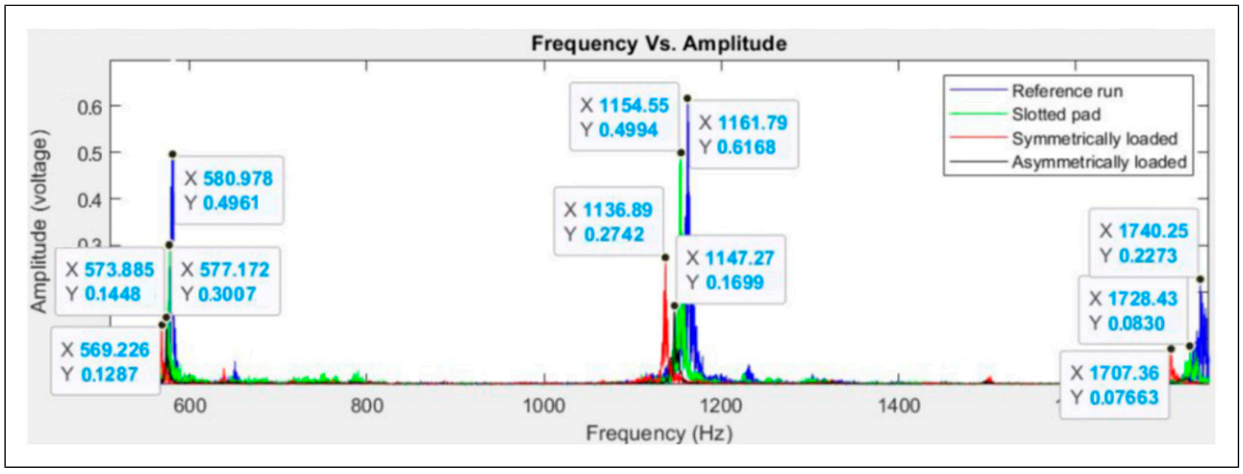

Figure 8. Brake noise audio recording of the reference run in blue, the slotted run in green, the symmetrically loaded run in red, and the asymmetrically loaded run in black. Amplitude is in volts, as recorded by the smartphone connected to the BOYA BY-M1 microphone.

Table 4. Comparison of the brake noise magnitude and frequency of the radially slotted brake pads with the reference run.

	Reference		Slotted		
Brake noise	Frequency (Hz) (average)	Magnitude (V) (average)	Frequency (Hz) (average)	Magnitude (V) (average)	% magnitude reduction
Low frequency	580.8	0.48339	581.2	0.29646	38.7
Middle frequency	1162.6	0.61555	1159.1	0.50150	18.5
High frequency	1740.8	0.21249	1730.3	0.09103	57.2

Table 5. Comparison of the brake noise magnitude and frequency of the symmetrical loading of the rotor with the reference run.

	Reference		Symmetrically loaded		
Brake noise	Frequency (Hz) (average)	Magnitude (V) (average)	Frequency (Hz) (average)	Magnitude (V) (average)	% magnitude reduction
Low frequency	580.8	0.48339	568.4	0.12103	75
Middle frequency	1162.6	0.61555	1138.4	0.27267	55.7
High frequency	1740.8	0.21249	1707	0.07888	63

Table 6. Comparison of the brake noise magnitude and frequency of the asymmetrical loading of the rotor with the reference run.

	Reference		Asymmetrically loaded		
Brake noise	Frequency (Hz) (average)	Magnitude (V) (average)	Frequency (Hz) (average)	Magnitude (V) (average)	% magnitude reduction
Low frequency	580.8	0.48339	574.4	0.13538	72
Middle frequency	1162.6	0.61555	1150.5	0.16693	73
High frequency	1740.8	0.21249	-	-	99.9

Of all the countermeasures evaluated in the present study, asymmetric loading performed the best at reducing brake noise magnitude. It eliminated high frequency vibrations completely, as shown in Figure 8 where there is no third peak for the asymmetric loading (in black). It also reduced the low and middle frequency magnitudes by nearly 75%. A comparison of the asymmetrical loading run with the reference run is shown in Table 6.

11. Conclusion

The aim of this project was to gain insight into disc brake noise and devise ways to reduce it. We used the test bench setup consisting of the brake test machine designed by Schmidt Engineering GmbH to run the bicycle in the laboratory settings. We collected brake noise audio recordings via a microphone placed close to the pad-rotor interface, and we used PSV-400 vibrometer to perform an experimental modal analysis of the brake assembly.

Audio recordings revealed that brake noise that we hear is in just three peak frequencies of about 580 Hz, 1160 Hz, and 1740 Hz. The middle and high-frequency noises are the most annoying to the human ear because of human hearing being the most sensitive in the regions of 1–4 kHz.

We found that vibrations originate at the pad-rotor interface and travel to the front fork, and that some parts vibrated at a velocity of as high as 1.5 mm/s.

We analysed the brake assembly with finite elements and compared the results to the experimental data to validate it. The finite element model was successfully able to predict the mode shapes and Eigenfrequencies of the real-life brake system. The frequencies from the simulations and the experimental investigation had a maximum difference of only 45 Hz and no difference in the mode shapes.

In addition to this, the finite element model also predicted the presence of in-plane vibration modes in a middle frequency, which the laser Doppler vibrometer was not able to detect. We saw doublet modes that could lead to flutter instability and intermediate mode lock-in during the finite element analysis.

Based on the observations from the experiments and simulations, we tested three countermeasures (a radial slot in the brake pads, a symmetrically loaded rotor, and an asymmetrically loaded rotor) both experimentally and analytically.

We made a radial slot into the frictional lining to improve heat management and found that it managed to reduce the low frequency, middle frequency, and high-frequency magnitudes by 38.7%, 18.5%, and 57.2%, respectively.

We added mass to the rotor symmetrically to address intermediate mode lock-in between the pads and the rotor, and it successfully lowered the vibration magnitudes and frequencies. We observed a decrease of 75% in low frequency magnitude, 55.7% in middle frequency magnitude, and 63% in the high-frequency magnitude.

Finally, we added mass to the rotor asymmetrically to address the doublet modes. This completely suppressed the high-frequency noise, and decreased the low frequency magnitude by 72%, and the middle frequency magnitude by 73%.

Of the three countermeasures that we tested, asymmetric loading worked the best in reducing the magnitude and frequency of the vibrating structure.

Acknowledgements

Royal Dutch Gazelle provided bicycles, test equipment, and working space.

Declaration of Conflicting Interests

The author(s) declared the following potential conflicts of interest with respect to the research, authorship, and/or publication of this article: No person or entity has or had any financial stake in this research nor its results, and all data collected has been shared freely between participants in this research. Ajaypal Singh worked as an unpaid intern at Royal Dutch Gazelle, conducted research there for his TU Delft master's thesis, and Hans Vreman was his supervisor. Hans Vreman works as a Mechanical Engineer at Royal Dutch Gazelle. Andrew Dressel worked at TU Delft for a 1-year post-doc funded by the TKI/ClickNL 'De Fiets van de Toekomst' grant and acted as Mr Singh's day-to-day supervisor at TU Delft. Jason Moore is an Assistant Professor at TU Delft and was Ajaypal Singh's thesis advisor.

Funding

The author(s) disclosed receipt of the following financial support for the research, authorship, and/or publication of this article: This work was supported by the The TKI/ClickNL 'De Fiets van de Toekomst' grant provided funding.

ORCID iDs

Ajaypal Singh https://orcid.org/0009-0009-0473-2739
Andrew E Dressel https://orcid.org/0000-0003-0322-9815
Jason K Moore https://orcid.org/0000-0002-8698-6143

References

Abendroth H and Wernitz B (2000) The integrated test concept: dyno - vehicle, performance – noise. SAE Technical Paper 2000-01-2774.

Akay A (2002) Acoustics of friction. *Journal of the Acoustical Society of America* 111(4): 1525–1548.

Allgaier R, Gaul L, Keiper W, et al. (1970) Mode lock-in and friction modelling. *WIT Transactions on Engineering Sciences* 24.

Budinsky T, Brooks P and Barton D (2021) A new prototype system for automated suppression of disc brake squeal. *Proceedings of the Institution of Mechanical Engineers - Part D: Journal of Automobile Engineering* 235(5): 1423–1433.

Chan SN, Mottershead JE and Cartmell MP (1994) Parametric resonances at subcritical speeds in discs with rotating frictional

loads. *Proceedings of the Institution of Mechanical Engineers - Part C: Journal of Mechanical Engineering Science* 208(6): 417–425. DOI: 10.1243/PIME_PROC_1994_208_147_02.

Lang AM, Newcomb TP and Brooks PC (1993) Brake squeal-the influence of rotor geometry. In: *Proceedings of the Institution of Mechanical Engineers. Braking of Road Vehicles*. London, UK: International Conference.

Montgomery DC (2017) *Design and Analysis of Experiments*. 8th edition. Hoboken: Wiley.

Nishlwakl M, Harada H, Okamura H, et al. (1989) Study on disc brake squeal. SAE Technical Paper 890864.

Polytec (2024) Modal analysis. Available at: https://www.polytec.com/us/vibrometry/modal-analysis (accessed 23 February 2024).

Rabinowicz E (1965) *Friction and Wear of Materials*. New York: Wiley, 94–101.

Singh A (2022) *Investigation of the Chatter and Squeal Phenomenon in Bicycle Disc Brakes*. Master's Thesis. The Netherlands: Delft University of Technology.

Wu-Bavouzet F, Clain-Burckbuchler J, Buguin A, et al. (2007) Stick-slip: wet versus dry. *The Journal of Adhesion* 83(8): 761–784. DOI: 10.1080/00218460701586178.